

Schematic model based on two-center shell model for neutron sub-Coulomb transfer in colliding deformed and oriented ^{24}Mg nuclei

Thomas Kraft

Institut für Theoretische Physik, Justus-Liebig-Universität, Giessen, Germany

Raj K. Gupta

Physics Department, Panjab University, Chandigarh-160014, India

Werner Scheid

Institut für Theoretische Physik, Justus-Liebig-Universität, Giessen, Germany

(Received 9 October 1990)

By using a two-state approximation, a time-dependent semiclassical theory is developed for the sub-Coulomb transfer of a neutron between two deformed and arbitrarily oriented nuclei. This theory yields the transfer probability as a function of the energy splitting of molecular single-particle states which are degenerate for large internuclear separations. We apply this theory schematically to central collisions of ^{24}Mg on ^{24}Mg using a two-center shell model and considering only the three low-lying states $1s_{1/2}$, $1p_{3/2}(\Omega=\frac{1}{2})$, and $1p_{3/2}(\Omega=\frac{3}{2})$ of the deformed ^{24}Mg nucleus. Transfer probabilities are calculated as a function of the orientation of the deformed ^{24}Mg nuclei with respect to the internuclear axis and compared with phenomenological probabilities depending exponentially on the minimum center-to-center and surface-to-surface distances. The transfer probabilities from the $1s_{1/2}$ and $1p_{3/2}(\Omega=\frac{1}{2})$ states seem to support the exponential dependence on the minimal surface-to-surface distance.

I. INTRODUCTION

In recent years, the problem of a single-neutron transfer in colliding heavy and deformed nuclei has been of great interest, both experimentally and theoretically. In the first experiment of Wirth *et al.*¹ for ^{238}U on ^{238}U at energies both near and well below the Coulomb barrier, the measured excitation function and angular distribution for the one-neutron-transfer product ^{239}U did not fit the predictions of the semiclassical theory of neutron transfer (SCTT).^{2,3} Since the SCTT has been quite successful for nucleon-transfer reactions using light heavy-ion beams of spherical nuclei, it was considered⁴ that the deformations and orientations of the colliding nuclei could be responsible for the disagreement between the theory and experiment. Gupta *et al.*⁴ calculated the classical Rutherford trajectories for deformed and oriented nuclei and incorporated these effects in the SCTT. The preliminary analysis⁵ of the neutron-transfer data of another reaction, namely, of ^{238}U on ^{197}Au , involving a deformed nucleus is found to be more consistent with the SCTT for spherical nuclei. The SCTT is put to a still more severe test by the reported data⁶ of sub-Coulomb neutron transfer for $^{58}\text{Ni} + \text{Sm}$ isotopes. The deformation effects of Sm isotopes are more than evident in these data. Theoretically, two other schematic model calculations are available.^{7,8} In the first one,⁷ seeing the effect of a "shoulder" in the interaction potential was attempted, which gives rise to larger contact times. The second calculation,⁸ based on a simple semiclassical analysis, uses an analytical formula for a one-neutron-transfer cross section that contains ab-

sorption effects. As expected and already shown by Wirth *et al.*,¹ the absorption effects are important only for higher incident energies near and above the barrier.

In the SCTT for spherical nuclei, the differential cross section contains, in addition to the product of the Rutherford cross section and spectroscopic factor, an exponential dependence on the center-to-center distance at the point of closest approach. This theory was extended⁴ to collisions between deformed and oriented nuclei by assuming two simple hypotheses: (a) the transfer cross section still has an exponential factor depending on the minimal center-to-center distance at the point of closest approach, or (b) the minimum surface-to-surface distance at the point of closest approach determines the exponent of transfer cross section. The two hypotheses, which yield the same result for spherical nuclei, affect the cross section in a reverse manner. The spectroscopic factor was assumed to be independent of the deformation and orientation of the nuclei. The application of these two hypotheses to the neutron-transfer data of the reaction $^{238}\text{U} + ^{238}\text{U}$ did not allow us to say which of the two hypotheses is better.

In this paper, we calculate the one-neutron-transfer probability between two deformed and arbitrarily oriented nuclei microscopically with the help of a two-center shell model. Assuming central collisions, we use the time-dependent semiclassical reaction theory which, in first order, gives the transfer probability in terms of single-particle separation energies. In the deformed two-center shell model, such a level separation depends on both relative distance and the orientations of the nuclei.

Such a connection between the two-center shell model and the nucleon-transfer probability could, in turn, help us to distinguish between the above-mentioned two hypotheses of minimum center-to-center and surface-to-surface distances. For calculating the single-particle energy separation as functions of relative distance and orientations of the nuclei, we use the two-center shell model of Nuhn *et al.*,⁹ worked out for arbitrarily oriented major axes of the deformed nuclei. For an application of our method, we have chosen the light system $^{24}\text{Mg} + ^{24}\text{Mg}$, since the $^{238}\text{U} + ^{238}\text{U}$ system involves too much computer time.

Section II gives the time-dependent, semiclassical reaction theory, which relates the single-neutron-transfer probability to the splitting of single-particle energies of the corresponding states. The two-center shell model (TCSM) for the $^{24}\text{Mg} + ^{24}\text{Mg}$ system is described in Sec. III and is used to calculate the neutron-transfer probability in Sec. IV. Our calculations of parametrizing the TCSM energy splitting and of the neutron-transfer probability and their comparison with calculations using the two hypotheses of minimum center-to-center and surface-to-surface distances are given in Sec. V. Finally, a summary and discussion of our results are presented in Sec. VI.

II. SEMICLASSICAL THEORY FOR SUB-COULOMB NEUTRON TRANSFER IN TWO-STATE APPROXIMATION

For collisions at energies below the barrier, the deformed nuclei are taken to move on classical Coulomb trajectories.^{4,10} In order to treat the neutron transfer, we restrict ourselves to a two-state approximation for reasons of simplicity and consider that the neutron is transferred between these two specific states. Then, this neutron moves in a combined two-center potential of the deformed nuclei and its motion is described by the time-dependent Schrödinger equation

$$H(\mathbf{r}, \mathbf{R}(t), \Omega_1(t), \Omega_2(t))\psi(\mathbf{r}, t) = i\hbar \frac{\partial \psi(\mathbf{r}, t)}{\partial t}. \quad (1)$$

Here, H is the Hamiltonian of the two-center shell model with a two-center potential $V = V^{(1)} + V^{(2)}$, where $V^{(1)}$ is concentrated around nucleus 1 and $V^{(2)}$ around nucleus 2. \mathbf{R} is the relative distance vector between the nuclear centers of masses and $\Omega_{i=1,2}$ are Euler angles for the orientations of the nuclear intrinsic axes. The coordinate \mathbf{r} refers to the single neutron and is measured from the center of mass of the system.

Now, using the two-state approximation in the method of linear combination of nuclear orbitals, i.e., the LCNO method, which is similar to the linear combination of atomic orbitals (LCAO) method in atomic physics,¹¹ the neutron wave function $\psi(\mathbf{r}, t)$ can be expanded in terms of the two states of the separated nuclei:¹²

$$\psi = c_1(t) \exp(-iE_1 t / \hbar) \phi_1(\mathbf{r} - p\mathbf{R}) + c_2(t) \exp(-iE_2 t / \hbar) \phi_2(\mathbf{r} + q\mathbf{R}) \quad (2)$$

with $p = A_2 / (A_1 + A_2)$ and $q = A_1 / (A_1 + A_2)$. In this

wave function we assume the relative distance and the orientation of the nuclei as slowly varying in time and neglect the time derivatives with respect to these variables. Inserting the above wave function into a variational principle, as explained in Ref. 11, we obtain the following coupled differential equations for the time-dependent coefficients $c_i(t)$:

$$i\hbar \dot{c}_1 = \frac{V_{12}^{(1)} - S_{12} V_{22}^{(1)}}{1 - |S|^2} c_2 \exp(i\omega_{12} t) + \frac{V_{11}^{(2)} - S_{12} V_{21}^{(2)}}{1 - |S|^2} c_1, \quad (3)$$

$$i\hbar \dot{c}_2 = \frac{V_{21}^{(2)} - S_{21} V_{11}^{(2)}}{1 - |S|^2} c_1 \exp(-i\omega_{12} t) + \frac{V_{22}^{(1)} - S_{21} V_{12}^{(1)}}{1 - |S|^2} c_2$$

with

$$\hbar\omega_{12} = E_1 - E_2. \quad (4)$$

The overlap integrals of the two basis functions are defined as

$$S_{12} = \langle \phi_1(\mathbf{r} - p\mathbf{R}) | \phi_2(\mathbf{r} + q\mathbf{R}) \rangle, \quad (5)$$

$$|S|^2 = S_{12} S_{21},$$

and the matrix elements

$$V_{11}^{(2)} = \langle \phi_1(\mathbf{r} - p\mathbf{R}) | V^{(2)} | \phi_1(\mathbf{r} - p\mathbf{R}) \rangle, \quad (6)$$

$$V_{21}^{(2)} = \langle \phi_2(\mathbf{r} + q\mathbf{R}) | V^{(2)} | \phi_1(\mathbf{r} - p\mathbf{R}) \rangle$$

with analogous expressions for $V_{12}^{(1)}$ and $V_{22}^{(1)}$.

Then, with the help of the following transformations:

$$c_1 = d_1 \exp \left[-i \int_0^t \alpha(t') dt' \right], \quad (7)$$

$$c_2 = d_2 \exp \left[-i \int_0^t \beta(t') dt' \right],$$

where

$$\hbar\alpha(t) = \frac{V_{11}^{(2)} - S_{12} V_{21}^{(2)}}{1 - |S|^2}, \quad \hbar\beta(t) = \frac{V_{22}^{(1)} - S_{21} V_{12}^{(1)}}{1 - |S|^2},$$

and shorthand notations

$$\omega = (\tilde{E}_1 - \tilde{E}_2) / \hbar, \quad \tilde{E}_1 = E_1 + \hbar\alpha, \quad \tilde{E}_2 = E_2 + \hbar\beta, \quad (8)$$

$$X_{12}^{(1)} = \frac{V_{12}^{(1)} - S_{12} V_{22}^{(1)}}{1 - |S|^2}, \quad X_{21}^{(2)} = \frac{V_{21}^{(2)} - S_{21} V_{11}^{(2)}}{1 - |S|^2},$$

we get the following coupled equations from Eq. (3):

$$i\hbar \dot{d}_1 = X_{12}^{(1)} \exp \left[i \int_0^t \omega dt' \right] d_2, \quad (9)$$

$$i\hbar \dot{d}_2 = X_{21}^{(2)} \exp \left[-i \int_0^t \omega dt' \right] d_1.$$

The coupled equations have stationary adiabatic solutions with the eigenvalues

$$E^\pm = (\tilde{E}_1 + \tilde{E}_2) / 2 \pm [(\tilde{E}_1 - \tilde{E}_2)^2 / 4 + X_{12}^{(1)} X_{21}^{(2)}]^{1/2}. \quad (10)$$

These are the energies of the molecular two-center states in the two-state approximation.

The probability for the neutron to go from state 1 at time $t = -\infty$ to state 2 at time $t = \infty$ is obtained by solv-

ing Eqs. (9) under the initial conditions $d_1(t=-\infty)=1$ and $d_2=0$. In the time-dependent perturbation calculation of first order we get, for $d_2(t)$,

$$d_2(t) = \frac{1}{i\hbar} \int_{-\infty}^t X_{21}^{(2)}(t') \exp \left[-i \int_0^{t'} \omega dt'' \right] dt' \quad (11)$$

which yields the transfer probability P_{12} from state 1 to state 2:

$$P_{12} = |d_2(t=\infty)|^2. \quad (12)$$

For a general collision, the probability P_{12} cannot be related to the energies given in Eq. (10). However, for equal nuclei with symmetric orientations of the intrinsic axes with respect to the center of mass and for the same neutron states, we can derive a simple relation. In this case we have

$$X_{12}^{(1)} = X_{21}^{(2)*} = \exp(i\chi) X \quad (X > 0), \quad (13)$$

$$E_1 = E_2, \quad \tilde{E}_1 = \tilde{E}_2, \quad \omega = 0, \quad (14)$$

$$E^+ - E^- = 2X. \quad (15)$$

Then, the probability P_{12} for the transfer of a neutron between two equal states bound in two equal nuclei with a symmetric orientation of the system with respect to the center of mass becomes

$$P_{12} = \left| \frac{1}{2} \int_{-\infty}^{\infty} \exp(i\chi)(E^+ - E^-) dt / \hbar \right|^2. \quad (16)$$

For the following let us assume $d\chi/dt=0$. Equation (16) gives the transfer probability as an integral over the splitting of energies of two molecular states which are energetically degenerate at large internuclear distances ($E_1=E_2$). Therefore Eq. (16) has the advantage that we can simply calculate the probability for neutron transfer by reading the energy difference out of a two-center level diagram of equal deformed nuclei with symmetric orientations of the intrinsic axes. We notice that the energy difference $E^+ - E^-$ depends on time or equivalently on the internuclear distance in heavy-ion collisions. In actual calculations the spectroscopic factors must be regarded too.

III. TWO-CENTER SHELL MODEL FOR THE $^{24}\text{Mg} + ^{24}\text{Mg}$ SYSTEM

In this section, we give an overview of the two-center shell model of Nuhn *et al.*⁹ for arbitrarily oriented nuclei. The Hamiltonian of the problem is

$$H = -\frac{\hbar^2}{2M} \nabla^2 + V(\mathbf{r}, \mathbf{p}, \mathbf{s}), \quad (17)$$

where the two-center potential V is a linear superposition of two potentials, including the spin-orbit potentials

$$V(\mathbf{r}, \mathbf{p}, \mathbf{s}) = \sum_{i=1}^2 [V_i + C_i(\nabla V_i \times \mathbf{p}) \cdot \mathbf{s}]. \quad (18)$$

The potentials V_i are centered on the internuclear axis at $z=Z_1$ and Z_2 with the two-center distance given by $R=|Z_1-Z_2|$. They are assumed to be of Gaussian func-

tional form with ellipsoidal equipotential surfaces

$$V_i = -V_{0i}(1+a_i u_i^2) \exp(-u_i^2) \quad (19)$$

with

$$u_i^2 = (\delta_{i1}^2 x_i'^2 + \delta_{i2}^2 y_i'^2 + \delta_{i3}^2 z_i'^2) / \lambda_i^2. \quad (20)$$

Here, $\delta_{i\mu}$ ($\mu=1,2,3$) are the deformation parameters and x_i', y_i', z_i' with $i=1,2$ are the coordinates of the two intrinsic coordinate systems centered at $z=Z_1$ and Z_2 , respectively, and rotated by the Euler angles $\Omega_i=(\phi_i, \theta_i, \psi_i)$ as shown in Fig. 1.

In the case of the $^{24}\text{Mg} + ^{24}\text{Mg}$ system we have two equal nuclei with rotationally symmetric shapes about the intrinsic z_i' axes. Therefore, we can set the parameters of the potential as equal:

$$V_{01} = V_{02} = V_0, \quad a_1 = a_2 = a, \quad \lambda_1 = \lambda_2 = \lambda, \quad (21)$$

$$\delta_{1\mu} = \delta_{2\mu}, \quad C_1 = C_2 = -2\kappa / (M\hbar\omega_0),$$

where $\hbar\omega_0 = 41 A^{-1/3}$ MeV and κ is the spin-orbit parameter. The deformation parameters $\delta_{i\mu}$ of the rotationally symmetric shapes can be parametrized as in the Nilsson model:¹³

$$\delta_{i1}^2 = \delta_{i2}^2 = (1 + \frac{2}{3}\delta) / N, \quad (22)$$

$$\delta_{i3}^2 = (1 - \frac{4}{3}\delta) / N$$

with $N = (1 + \frac{2}{3}\delta)^{2/3} (1 - \frac{4}{3}\delta)^{1/3}$.

The parameters V_0 , a , λ , κ , and δ depend on the relative distance. They are determined from the single-particle spectra for neutrons of ^{24}Mg and ^{48}Cr for $R \rightarrow \infty$ (separated nuclei) and $R \rightarrow 0$ (fused system), respectively, and interpolated in between. The interpolation is achieved by keeping the volume of a certain equipotential surface near the Fermi level constant for all values of R and Ω_i . Thus, a continuous and realistic two-center potential can be obtained for each relative distance R and orientations of the ^{24}Mg nuclei.

Table I gives the parameters of the potential for $R \rightarrow \infty$ and $R \rightarrow 0$ found by fitting single-particle energies

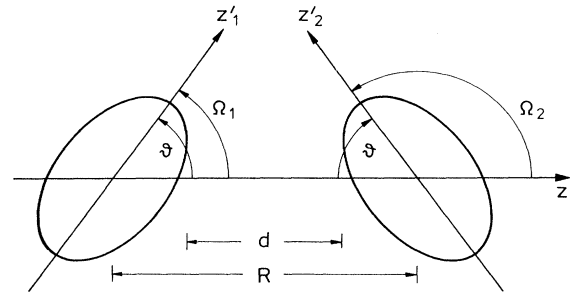


FIG. 1. Two prolate deformed equal nuclei with an orientation of the intrinsic symmetry axes to the internuclear axis defined by the Euler angles $\Omega_1=(0, \theta, 0)$ and $\Omega_2=(0, \pi - \theta, 0)$. The center-to-center distance is denoted by R and the shortest distance between the surfaces by d .

TABLE I. The potential parameters for ^{24}Mg and ^{48}Cr .

Parameter	^{24}Mg	^{48}Cr
V_0 (MeV)	48.0	24.83 (=49.66/2)
a	0.996	0.980
λ (fm)	2.79	3.5
κ	0.075	0.1
δ	0.35	0
$\hbar\omega$ (MeV)	11	9

of ^{24}Mg and ^{48}Cr near the Fermi level. For the spherically assumed ^{48}Cr nucleus, we took the neutron single-particle energies obtained by an interpolation of observed single-particle energies in ^{40}Ca and ^{56}Ni given in Ref. 14. The observed single-particle energies of ^{24}Mg are taken from Park *et al.*¹⁵ and are listed together with the calculated energies in Table II. The observed single-particle energies were obtained from the spectrum of ^{25}Mg interpreted by the strong coupling of the neutron motion to the deformed ^{24}Mg core and described in the framework of the Nilsson model and the aligned coupling scheme.¹⁶ The deformation parameter δ of the ^{24}Mg nucleus was set as $\delta=0.35$ in complete agreement with the intrinsic electric quadrupole moment of ^{25}Mg which has been determined to $Q_0=61.6\text{ efm}^2$ (Ref. 17). The electric quadrupole moment is given in terms of the semi-axes a and b of a spheroidal equipotential surface by

$$Q_0 = \frac{2}{5}Ze(a^2 - b^2) = \frac{4}{5}ZeR_0^2 \frac{\delta}{(1 + \frac{2}{3}\delta)^{1/3}(1 - \frac{4}{3}\delta)^{2/3}}, \quad (23)$$

where $R_0 = 1.25 A^{1/3}\text{ fm}$ is the nuclear radius.

The Hamiltonian (17) gets diagonalized with Nilsson wave functions as basis set. The oscillator frequencies are chosen as $\hbar\omega_{1\mu} = \hbar\omega\delta_{1\mu}$ with $\mu=1, 2, 3$. The value of $\hbar\omega$ is obtained by a minimalization procedure. For ^{24}Mg and

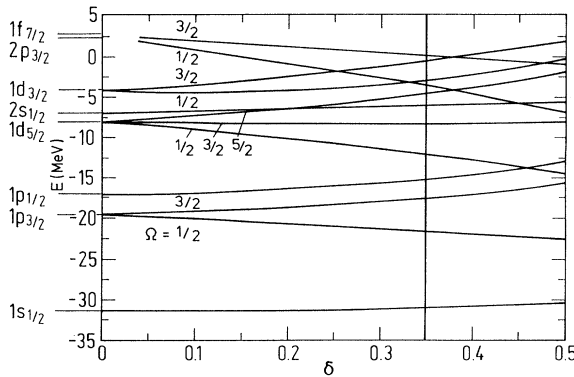


FIG. 2. The single-particle energies for ^{24}Mg calculated as a function of the deformation parameter δ . The magnetic quantum numbers of the states are indicated. A deformation of $\delta=0.35$, shown by the vertical line, is used in the further calculations.

TABLE II. Observed and calculated single-particle energies for ^{24}Mg . The observed single-particle energies are taken from Park *et al.* (Ref. 15). Ω is the magnetic quantum number.

State	E (obs.) (MeV)	E (calc.) (MeV)
$2s_{1/2}(\Omega=\frac{1}{2})$	-6.82	-6.27
$1d_{5/2}(\Omega=\frac{5}{2})$	-6.47	-4.87
$1d_{3/2}(\Omega=\frac{3}{2})$	-4.88	-3.20
$1f_{7/2}(\Omega=\frac{7}{2})$	-3.48	-3.78

^{48}Cr we found $\hbar\omega=11$ and 9 MeV , respectively, also listed in Table I.

Figure 2 shows the eigenvalues calculated with the parameters for ^{24}Mg listed in Table I as a function of the deformation parameter δ . The calculated energies given in Table II belong to a deformation of $\delta=0.35$ in this figure. States with eigenvalues larger than zero are pseudostates for the continuum, since our basis set consists only of bound-state wave functions and, therefore, does not correctly describe continuum states.

The following studies are restricted to special orientations of the intrinsic axes. We only consider here configurations where the two nuclei are rotated around the y axis with Euler angles $\Omega_1=(0, \theta, 0)$ and $\Omega_2=(0, \pi - \theta, 0)$, as shown in Fig. 1. In Fig. 3 we show the two-center potential $V=V_1+V_2$ without the spin-orbit potential along the z axis for $R=10\text{ fm}$ and the nuclear orientations $\theta=0^\circ, 30^\circ, 60^\circ$, and 90° . We notice that the potential barrier lies lowest for $\theta=0^\circ$ when the overlap of the nuclei is largest. The equipotential surfaces in the x - z plane are illustrated in Fig. 4 for $\theta=0^\circ$ and 60° .

Finally, the single-particle energy spectra are plotted in Fig. 5 as a function of R for $\theta=0^\circ, 30^\circ, 60^\circ$, and 90° . We have shown here the lowest-lying molecular states which asymptotically approach the states $1s_{1/2}$, $1p_{3/2}(\Omega=\frac{1}{2})$, and $1p_{3/2}(\Omega=\frac{3}{2})$. The energies are fourfold degenerate

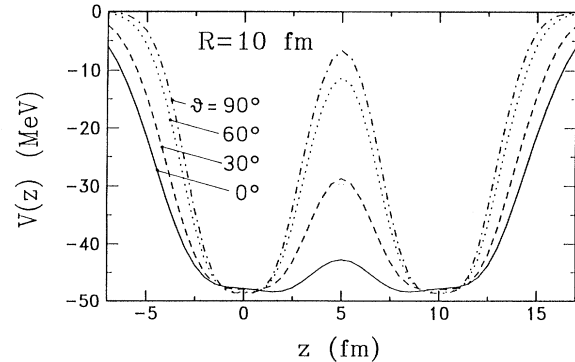


FIG. 3. The two-center potential $V(z)$ along the z axis for the $^{24}\text{Mg}+^{24}\text{Mg}$ system at an internuclear distance of $R=10\text{ fm}$ for different orientation angles $\theta=0^\circ$ (full curve), 30° (dashed curve), 60° (dotted curve), and 90° (dash-dotted curve).

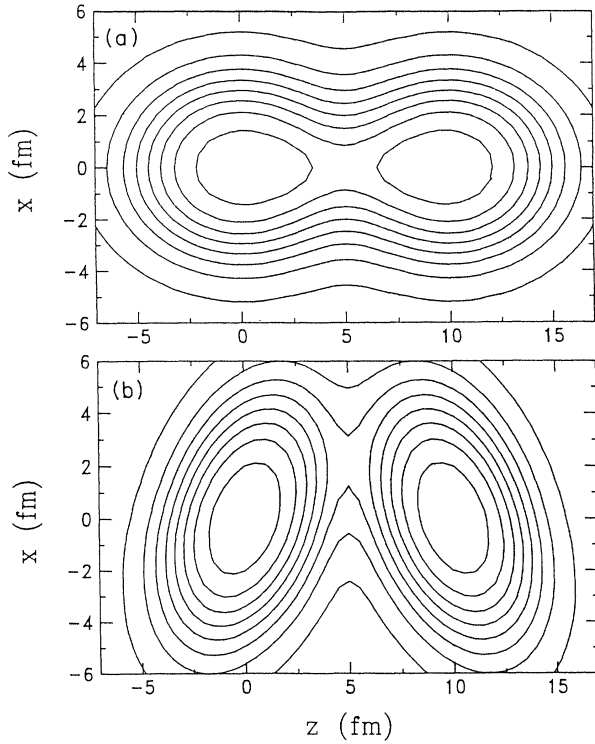


FIG. 4. Equipotential curves of the two-center potential for the $^{24}\text{Mg}+^{24}\text{Mg}$ system at $R=10$ fm for the orientation angles (a) $\theta=0^\circ$ and (b) $\theta=60^\circ$. The equipotential curves are shown for -45 MeV to -3 MeV in steps of 6 MeV.

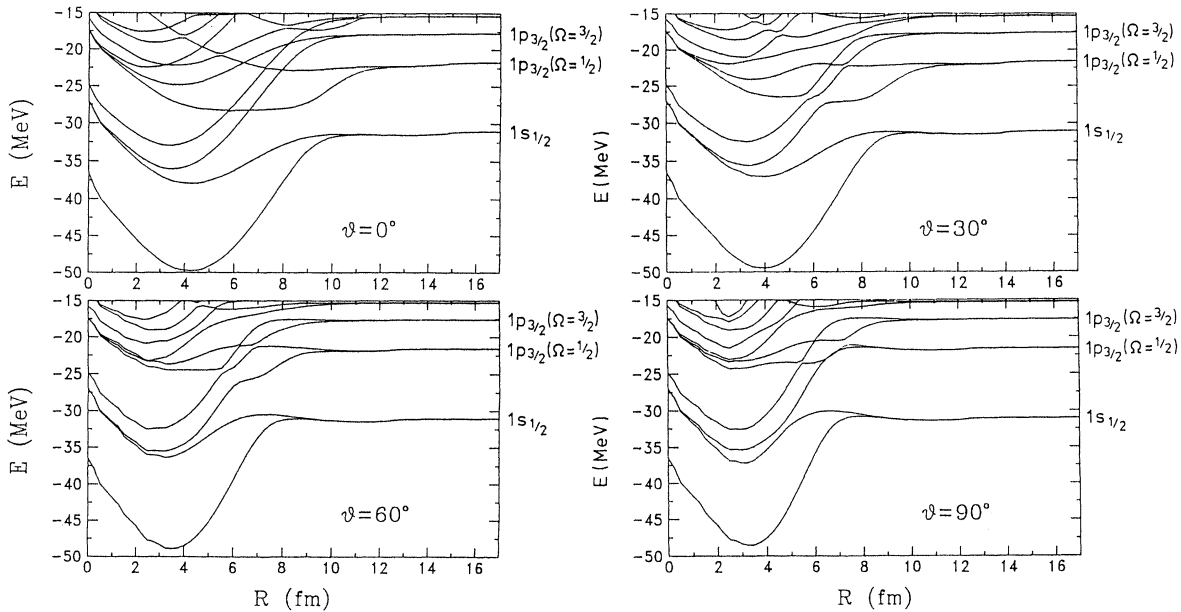


FIG. 5. Two-center level diagram for the $^{24}\text{Mg}+^{24}\text{Mg}$ system as a function of the internuclear distance R for different orientation angles $\theta=0^\circ, 30^\circ, 60^\circ,$ and 90° .

for $R \rightarrow \infty$ and split into twofold degenerate energies E^+ and E^- for finite values of R . Exactly such states with a symmetry with respect to the middle plane have been considered for the neutron transfer in Sec. II. In the following sections we will discuss the neutron transfer in a schematic model by using the two-center level diagram of Fig. 5.

IV. TWO-CENTER SHELL MODEL NEUTRON-TRANSFER PROBABILITY

For simplicity, we limit our calculations to the central collisions of ^{24}Mg on ^{24}Mg with symmetric orientations of the deformed ^{24}Mg nuclei as shown in Fig. 1. We assume that the orientation angle θ does not change during the collision. Such a change is shown to be small for heavy deformed nuclei.¹⁰ The relative motion of the nuclei is classically described by a Coulomb potential acting between the deformed nuclei and depending on the orientation angle θ :

$$V_C(R, \theta) = \frac{(Ze)^2}{R} + \frac{Ze}{R^3} Q_0 P_2(\cos\theta). \quad (24)$$

Using the energy-conservation relation

$$E_{\text{c.m.}} = \frac{1}{2}\mu\dot{R}^2 + V_C(R, \theta), \quad (25)$$

we can express the neutron-transfer probability (16) (with $\dot{\chi}=0$) as an integral over the relative distance R :

$$P_{12} = \frac{1}{4} \left| 2 \int_{R_{\text{min}}}^{\infty} (E^+ - E^-) dR / (\dot{R}\hbar) \right|^2, \quad (26)$$

where R_{min} is the relative distance at the classical turning

point, which is approximately given as

$$R_{\min} = \frac{(Ze)^2}{E_{c.m.}} + \frac{E_{c.m.}}{(Ze)^3} Q_0 P_2(\cos\theta). \quad (27)$$

The energy difference $\Delta E = E^+ - E^-$ in Eq. (26) decreases exponentially for touching configurations and larger relative distances as can be seen in Fig. 5. There-

$$P_{12} = \frac{A^2(\theta)\mu}{2(Ze)^2} \left| \int_{R_{\min}}^{\infty} \frac{\exp[-\alpha(\theta)R] dR}{R [1/R_{\min} - 1/R + (Q_0 P_2 / Ze)(1/R_{\min}^3 - 1/R^3)]^{1/2}} \right|^2. \quad (29)$$

After some minor neglect in the denominator we finally get the expression

$$P_{12} = \frac{\mu}{2(Ze)^2} R_{\min} A^2(\theta) \times \exp[-2\alpha(\theta)R_{\min}] [\exp(G)K_0(G)]^2 \quad (30)$$

with

$$G = \frac{1}{2}\alpha(\theta)R_{\min} \left[1 + \frac{3Q_0}{ZeR_{\min}} P_2(\cos\theta) \right]. \quad (31)$$

K_0 is the modified Bessel function of zero order.¹⁸ For $G > 2$, we can already use the asymptotic expression¹⁸

$$\exp(G)K_0(G) = [\pi/(2G)]^{1/2}. \quad (32)$$

For central collisions of spherical nuclei ($Q_0 = 0$), one obtains, from Eqs. (30)–(32) with $R_{\min} = (Ze)^2/E_{c.m.} = D$,

$$P_{12}^{\text{sph}} = \frac{\pi}{2} \frac{\mu}{(Ze)^2} \frac{A^2}{\alpha} \exp(-2\alpha D). \quad (33)$$

This is an interesting result. Equation (33) is exactly the formula for the transfer probability derived in the SCTT theory^{2,3} if one associates A to the dimensionless factor C_{AB} , also containing the spectroscopic quantities, and α to the wave number of the bound neutron: $\alpha = (2M\epsilon/\hbar^2)^{1/2}$, where ϵ is the binding energy of the single-particle state.

In Ref. 4 we studied the neutron transfer between deformed nuclei under two different hypotheses: (a) Assuming that the neutron-transfer probability depends on the minimum center-to-center distance R_{\min} , we set the probability in central collisions as

$$P_{12}^R(\theta) = P_R \exp[-2\alpha R_{\min}(\theta)]. \quad (34)$$

(b) Since the sub-Coulomb neutron transfer is a tunneling process through the potential barrier, the minimum distance d_{\min} between the nuclear surfaces is a very important quantity. Therefore, we investigated a second expression for the transfer probability in central collisions:

$$P_{12}^d(\theta) = P_d \exp[-2\alpha d_{\min}(\theta)], \quad (35)$$

where the minimum distance between the nuclear surfaces is given for the orientation of the nuclei shown in Fig. 1:

$$d_{\min}(\theta) = R_{\min}(\theta) - 2(a^2 \cos^2\theta + b^2 \sin^2\theta)^{1/2}. \quad (36)$$

fore, we introduce the following ansatz:¹²

$$\Delta E = \hbar A(\theta) \exp[-\alpha(\theta)R]/R \quad (28)$$

with orientation and state-dependent constants A and α , which will be determined from the two-center level diagram. Inserting Eq. (28) into Eq (26) and using Eqs. (24), (25), and (27), we obtain, for the probability,

Here, a and b denote the major and minor semi-axes of the ellipsoidal surfaces of the nuclei, respectively.

In order to compare the probabilities P_{12} , P_{12}^R and P_{12}^d as functions of θ , we set these probabilities equal at an angle $\theta = \theta_0 = 54.7^\circ$, where $P_2(\cos\theta)$ vanishes. In this case we have the following formulas for the probabilities P_{12}^R and P_{12}^d :

$$P_{12}^R(\theta) = P_{12}(\theta_0) \exp\{-2\alpha_0[R_{\min}(\theta) - D]\}, \quad (37)$$

$$P_{12}^d(\theta) = P_{12}(\theta_0) \times \exp\{-2\alpha_0[d_{\min}(\theta) - d_{\min}(\theta_0)]\} \quad (38)$$

with $\alpha_0 = \alpha(\theta_0)$, $D = R_{\min}(\theta_0) = (Ze)^2/E_{c.m.}$, and $P_{12}(\theta)$ calculated by the use of Eqs. (30) and (31).

Finally, we discuss the transfer probability as a quantity differential in the orientation angles of the intrinsic symmetry axes of the deformed nuclei. These angles are given by $\Omega_1 = (\theta_1, \phi_1)$ and $\Omega_2 = (\theta_2, \phi_2)$. The differential probability can be written as

$$dW = \frac{1}{16\pi^2} P(\Omega_1, \Omega_2) d\Omega_1 d\Omega_2, \quad (39)$$

where $P(\Omega_1, \Omega_2)$ is the transfer probability for a fixed orientation of the intrinsic symmetry axes. Since we have only derived the transfer probability for a special choice of Ω_1 and Ω_2 , namely, for $\Omega_1 = (\theta, \phi)$ and $\Omega_2 = (\pi - \theta, \phi)$, we can calculate the following triple-differential probability after integrating over $\phi = (\phi_1 + \phi_2)/2$:

$$\frac{d^3W}{d\theta_1 d\theta_2 d\phi_{12}} \Big|_{\theta_1 = \theta_2 = \theta, \phi_{12} = \phi_1 - \phi_2 = 0} = \frac{\sin^2\theta}{8\pi} P_{12}(\theta). \quad (40)$$

The factor $\sin^2\theta$ indicates the weight of the orientations of the intrinsic symmetry axes, which is largest for $\theta = 90^\circ$.

V. COMPARISON OF THE TRANSFER PROBABILITIES

In this section we want to compare the probabilities P_{12} , P_{12}^R and P_{12}^d in order to learn which of the hypotheses of minimum center-to-center and surface-to-surface distances is more useful for deformed nuclei. Since the energy difference $E^+ - E^-$ enters the probability, we need reliable two-center shell model calculations. They can be best done for the lowest levels as given in Fig. 5 for the $^{24}\text{Mg} + ^{24}\text{Mg}$ system. Therefore, we insert

the energy differences $E^+ - E^-$ of the lowest states, which are asymptotically characterized by the quantum numbers $1s_{1/2}$, $1p_{3/2}(\Omega = \frac{1}{2})$ and $1p_{3/2}(\Omega = \frac{3}{2})$, into the formula for P_{12} . This procedure should be understood as a valuable schematical model for the study of the neutron transfer and not interpreted as a realistic model for calculating probabilities in comparison with experimental data. In reality, all the chosen states are completely occupied by neutrons and, therefore, no neutron transfer could happen between these states. For similar reasons we have omitted a factor of 2 in Eq. (26) regarding the twofold degeneracy of the TCSM levels.

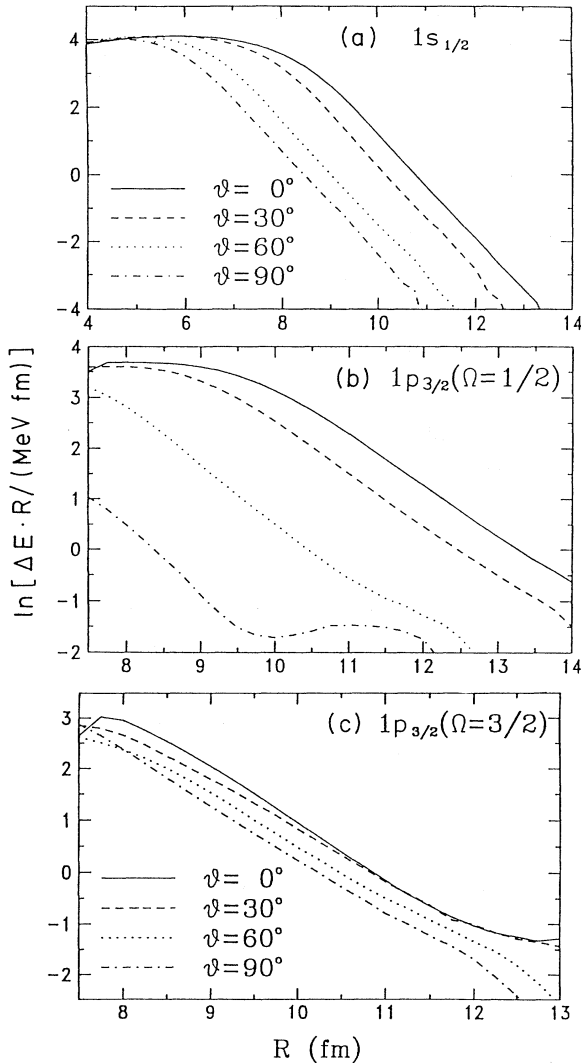


FIG. 6. The natural logarithm of the energy difference $\Delta E = E^+ - E^-$ multiplied by R as a function of R for the two-center states of $^{24}\text{Mg} + ^{24}\text{Mg}$ which are asymptotically classified by the quantum numbers (a) $1s_{1/2}$, (b) $1p_{3/2}(\Omega = \frac{1}{2})$, and (c) $1p_{3/2}(\Omega = \frac{3}{2})$. The full curves are calculated for an orientation angle $\theta = 0^\circ$, the dashed curves for $\theta = 30^\circ$, the dotted curves for $\theta = 60^\circ$, and the dot-dashed curves for $\theta = 90^\circ$.

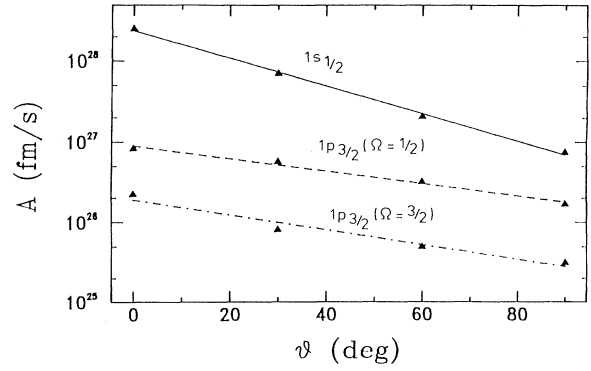


FIG. 7. The parameter A of Eq. (28) or (41) as a function of the orientation angle θ for the states denoted by $1s_{1/2}$ (full curve), $1p_{3/2}(\Omega = \frac{1}{2})$ (dashed curve), and $1p_{3/2}(\Omega = \frac{3}{2})$ (dot-dashed curve).

A. Parametrization of energy difference using TCSM

Equation (28) gives our proposed ansatz for the energy difference ΔE . Taking a natural logarithm on both sides of Eq. (28), we get

$$\ln[R \Delta E / (1 \text{ MeV fm})] = \ln[\hbar A / (1 \text{ MeV fm})] - \alpha R. \quad (41)$$

This is an equation of a straight line for

$$\ln[R \Delta E / (1 \text{ MeV fm})]$$

as a function of R with slope $-\alpha$ and intercept

$$\ln[\hbar A / (1 \text{ MeV fm})].$$

Figure 6 shows these plots for four different orientations, each for the three chosen TCSM states $1s_{1/2}$, $1p_{3/2}(\Omega = \frac{1}{2})$, and $1p_{3/2}(\Omega = \frac{3}{2})$. We notice that, for the relevant region of 7–13 fm, the curves are fairly straight lines for almost all the θ values. This proves our ansatz (28). For

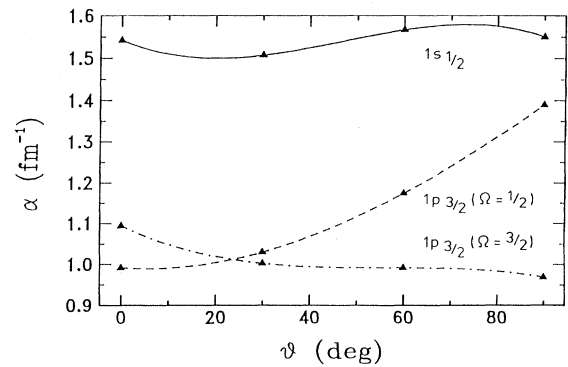


FIG. 8. The exponential parameter α defined in Eq. (28) or (41) as a function of the orientation angle θ for the states denoted by $1s_{1/2}$ (full curve), $1p_{3/2}(\Omega = \frac{1}{2})$ (dashed curve), and $1p_{3/2}(\Omega = \frac{3}{2})$ (dot-dashed curve).

larger relative distances we found deviations from the exponential law, because our limited basis set for the solution of the two-center shell model has only basis functions of Gaussian type.

Figures 7 and 8 show the obtained parameters A and α of the straight lines in Fig. 6 as functions of the orientation angle θ . We notice that the values of the parameter $A(\theta)$ fall on a straight line. The α values are very roughly connected to the binding energies of the considered states by $\alpha = (2M\varepsilon/\hbar^2)^{1/2}$ and can be represented by a polynomial of third degree.

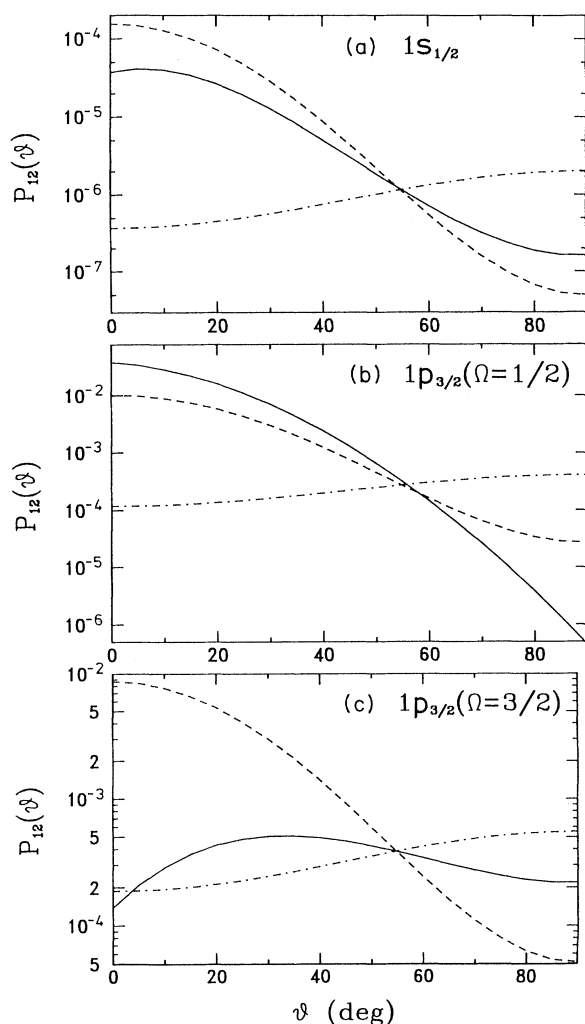


FIG. 9. The transfer probability in a central collision of ^{24}Mg on ^{24}Mg as a function of θ between various states of the $^{24}\text{Mg} + ^{24}\text{Mg}$ system denoted by (a) $1s_{1/2}$, (b) $1p_{3/2}(\Omega=1/2)$, and (c) $1p_{3/2}(\Omega=3/2)$. The incident energy is chosen as $E_{\text{c.m.}} = 18$ MeV. The full curves represent the transfer probabilities resulting from the energy differences in the two-center shell model. They are calculated with the parameters $A(\theta)$ and $\alpha(\theta)$ depicted in Figs. 7 and 8, respectively. The dot-dashed and dashed curves are the phenomenological transfer probabilities P_{12}^R and P_{12}^d as defined in Eqs. (37) and (38), respectively.

B. Results for the one-neutron-transfer probabilities

Figure 9 shows the calculated transfer probabilities P_{12} , P_{12}^R and P_{12}^d as functions of the orientation angle for an energy of $E_{\text{c.m.}} = 18$ MeV. We notice that for the states $1s_{1/2}$ and $1p_{3/2}(\Omega=1/2)$, the TCSM transfer probability P_{12} lies close to P_{12}^d , whereas, in the case of the state $1p_{3/2}(\Omega=3/2)$, P_{12} seems closer to P_{12}^R .

Finally, we have plotted in Fig. 10 the triple-differential probability (40) for equal orientations of the deformed ^{24}Mg nuclei. The major contribution to the transfer probability calculated with the two-center shell model arises around $\theta=25^\circ$ for the $1s_{1/2}$ and $1p_{3/2}(\Omega=1/2)$ states. The same behavior can be found for the triple-differential probability calculated with P_{12}^d in

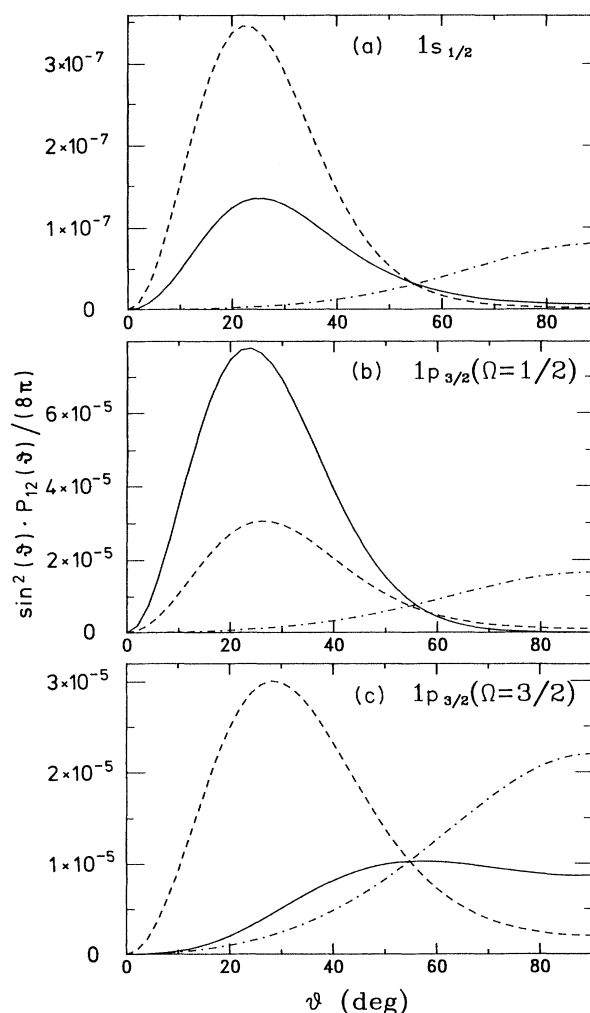


FIG. 10. The triple-differential probability as defined in Eq. (40) for the same collision as described in the caption of Fig. 9. The curves are obtained from the corresponding ones of Fig. 9 by multiplying them with a factor $\sin^2\theta/(8\pi)$. The notation of the curves is taken the same as in Fig. 9. We notice the linear scale of the transfer probability in contrast to the logarithmic scale applied in Fig. 9.

the case of all states, whereas the P_{12}^R probability peaks at $\theta=90^\circ$.

Figure 10 clearly demonstrates the main result of this paper. The three formulas for the probabilities P_{12} , P_{12}^R , and P_{12}^d yield very different results for the three considered states. The results for P_{12} depend sensitively on the single-particle states and, in general, cannot simply be simulated by the probabilities P_{12}^R and P_{12}^d based on the hypotheses of the minimal center-to-center and surface-to-surface distances.

VI. SUMMARY AND DISCUSSION OF OUR RESULTS

We have developed here a schematic model for one-neutron-transfer probability between two deformed and arbitrarily oriented ^{24}Mg nuclei. For this purpose we have used the two-center shell model of Nuhn *et al.*⁹ Our approach is schematic because only the lowest-lying states are considered and it is worked out only for the light system $^{24}\text{Mg}+^{24}\text{Mg}$. However, the experiments are made for heavier systems, like $^{238}\text{U}+^{238}\text{U}$ and $^{238}\text{U}+^{197}\text{Au}$, and actually the neutron transfer occurs between states near the Fermi surface. Also, we have used the adiabatic approximation of defining the neutron wave function. The validity of this scheme still remains to be tested in other nuclear phenomena, such as in multiple-particle transfer¹⁹ or in nuclear Landau-Zener effect.²⁰

The interesting result of this schematic model is that the one-neutron-transfer probability is related to the splitting of single-particle energy states, which depend on both relative separation and orientations of colliding nuclei. For the $^{24}\text{Mg}+^{24}\text{Mg}$ system, the energy separations calculated on the two-center shell-model basis satisfy an ansatz which gives a dependence of neutron-transfer

probability on the minimum center-to-center distance in the exponential. The resulting expression, simplified for the case of spherical nuclei, also gives the result of semiclassical theory of Breit and Ebel.² This proves the hypothesis of Gupta *et al.*⁴ that the exponential dependence of the single-neutron-transfer cross section on the minimum distance of closest approach is the same for both the spherical and deformed colliding nuclei.

Finally, we have tested the two proposed hypotheses of minimum center-to-center and surface-to-surface distances for central collisions. Calculations of transfer probabilities are made for the three lowest-lying shell-model states of the $^{24}\text{Mg}+^{24}\text{Mg}$ system. We find that two of these three chosen states seem to support the use of the minimum surface-to-surface distance hypothesis for deformed nuclei.

Comparing triple-differential probabilities, we recognize a great sensitivity of the transfer probability on the special single-particle state. These probabilities cannot be reproduced by the formulas for P_{12}^R and P_{12}^d . Therefore, we conclude that realistic microscopical calculations are needed in order to explore transfer probabilities between deformed nuclei. This could be done within the approach used here or, alternatively, one can work in a basis of separate inelastic channels of each of the deformed nuclei, combined with a sudden distorted-wave Born approximation (DWBA) type of transition for the neutron transfer. This method is used recently²¹ for particle-transfer studies between a deformed nucleus and a spherical nucleus. In turn, it would be interesting to compare the results of two such alternative approaches.

This work was supported by BMFT (06 GI 709) and GSI (Darmstadt).

¹G. Wirth, W. Brüche, M. Brügger, F. Wo, K. Sümmerer, F. Funke, J. V. Kratz, M. Lerch, and N. Trautmann, Phys. Lett. B **177**, 282 (1986).

²G. Breit and M. E. Ebel, Phys. Rev. **103**, 679 (1956); G. Breit, K. W. Chun, and H. G. Wahsweiler, *ibid.* **133**, B403 (1964); G. Breit, *ibid.* **135**, B1323 (1964).

³P. J. A. Buttle and L. J. B. Goldfarb, Nucl. Phys. **78**, 409 (1966); **A176**, 299 (1971).

⁴R. K. Gupta, R. Maass, and W. Scheid, Phys. Rev. C **37**, 1502 (1988).

⁵G. Wirth, W. Brüche, F. Wo, K. Sümmerer, F. Funke, J. V. Kratz, and N. Trautmann, *Lecture Notes in Physics* (Springer, Berlin, 1988), Vol. 317, p. 84.

⁶R. R. Betts, *Lecture Notes in Physics* (Springer, Berlin, 1988), Vol. 317, p. 93; C. N. Pass, P. M. Evans, A. E. Smith, L. Stuttge, R. R. Betts, J. S. Lilly, J. Simpson, A. N. James, and B. R. Fulton, Argonne National Laboratory Report PHY-6139-HI-89, 1989.

⁷D. P. Russel, W. T. Pinkston, and V. E. Oberacker, Phys. Lett. **158B**, 201 (1985).

⁸S. Landowne and G. Pollarolo, Phys. Lett. B **241**, 313 (1990).

⁹G. Nuhn, W. Scheid, and J. Y. Park, Phys. Rev. C **35**, 2146 (1987).

¹⁰R. K. Gupta and W. Scheid, Phys. Rev. C **36**, 1232 (1987); **40**, 1653 (1989).

¹¹M. R. C. McDowell and J. P. Coleman, *Introduction to the Theory of Ion-Atom Collisions* (North-Holland, Amsterdam, 1970), p. 141.

¹²R. K. Gupta, R. Maass, T. Kraft, and W. Scheid, in *Proceedings of the Sixth Adriatic International Conference on Nuclear Physics, Frontiers of Heavy-Ion Physics, Dubrovnik, 1987*, edited by N. Cindro *et al.* (World-Scientific, Singapore, 1987), p. 125.

¹³S. G. Nilsson, K. Dansk. Vidensk. Selsk. Mat.-Fys. Medd. **29**, No. 16 (1955).

¹⁴A. Bohr and B. R. Mottelson, *Nuclear Structure* (Benjamin, New York, 1969), Vol. 1.

¹⁵J. Y. Park, W. Scheid, and W. Greiner, Phys. Rev. C **6**, 1565 (1972).

¹⁶J. M. Eisenberg and W. Greiner, *Nuclear Theory* (North-Holland, Amsterdam, 1970), Vol. 1.

¹⁷P. M. Endt and C. van der Leun, Nucl. Phys. **A310**, 1 (1978).

¹⁸M. Abramowitz and I. A. Stegun, *Handbook of Mathematical Functions* (Dover, New York, 1972).

¹⁹C. Price, H. Esbensen, and S. Landowne, Phys. Lett. B **195**, 524 (1987).

²⁰J. Y. Park, W. Greiner, and W. Scheid, Phys. Rev. C **21**, 958 (1980).

²¹S. Landowne and C. H. Dasso, Phys. Lett. B **202**, 31 (1988).